

NRG approach to a quartet quantum-dot array connected to reservoirs: gate-voltage dependence of the conductance

Yunori Nisikawa and Akira Oguri

Department of Material Science, Osaka City University, Sumiyoshi-ku, Osaka 558-8585, Japan

(Dated: February 8, 2020)

We study the grand-state properties of a quartet quantum-dot array using a four-site Hubbard model connected to two non-interacting leads. We calculate the low-lying eigenstates by the numerical renormalization group (NRG) method and deduce the conductance from the fixed-point energy levels of the NRG in a wide parameter range. When the on-site energy ϵ_d that can be controlled by the gate voltage is varied, the conductance g shows wide minima and maxima alternatively, and the total number of electrons N_{el} in the four dots shows a staircase behavior for large Coulomb interaction U . The broad conductance maxima are caused by the Kondo effect and emerge for odd N_{el} , while the minima emerge for even N_{el} . The width of the minimum becomes quite large around half-filling owing to a tendency towards a development of a Mott-Hubbard insulating gap. These structures of the plateaus and valleys become gentle when the hybridization strength Γ between the chain and leads is increased. We also discuss the parallel conductance for the array connected to four non-interacting leads.

PACS numbers: 72.10.-d, 72.10.Bg, 73.40.-c

I. INTRODUCTION

The Kondo effect has recently been studied in novel systems such as quantum dots, quantum wires, and carbon nanotube. Early theoretical predictions^{1,2} have been successfully observed by the experiments,^{3,4} and in these years the interplay of various effects such as Aharonov-Bohm, Fano, Josephson, and Kondo effects have been studied.^{5,6,7,8,9,10,11} In these systems interesting behaviors due to inter-interactions are expected to be seen mainly at low temperatures, and recent progress in experimental technique seems to make it possible to realize these various situations in near future.

In order to study the transport properties through interacting systems at low temperatures, several numerical approaches have recently been examined.^{12,13,14} The Wilson numerical renormalization group (NRG) method which eliminates higher-energy states successively to obtain the low-lying energy states accurately,^{15,16,17} is one of the traditional methods, and has been applied successfully to single and double quantum dots.^{5,18,19} The NRG has recently been applied also to a series of three and four quantum dots.^{20,21} The low-temperature properties of these systems show a Fermi-liquid behavior,^{22,23} and at half-filling the conductance through even number of quantum dots decreases with increasing U ,²⁰ which reflects a tendency towards a development of a Mott-Hubbard insulating gap by the Coulomb interaction U . In contrast, for the series consisting of the odd number of quantum dots, the Kondo resonance emerges at the Fermi level contributes to tunneling current of the Unitary limit $g = 2e^2/h$. The conductance away from half-filling has also been studied precisely for triple quantum dots in a previous work.²¹

The purpose of the present work is to examine the transport through an array of four quantum dots away from half-filling. Using a four-site Hubbard chain con-

nected to two noninteracting leads, we study the dc conductance with varying the on-site potential ϵ_d , Coulomb interaction U , and Γ , which is the hybridization energy scale caused by the coupling between the leads and chain. At zero temperature, the conductance g and local charge N_{el} in the quantum dots are determined by the two phase shifts for the even and odd (s and p) partial waves owing to the Fermi-liquid properties.²¹ We calculate these two phase shifts from the fixed-point eigenvalues of NRG. Furthermore, from these phase shifts, we also deduce a parallel conductance through the four quantum dots connected transversely to four leads.

The results of the dc conductance show the typical Kondo plateaus of the Unitary limit $g \simeq 2e^2/h$ when the total number of electrons N_e in the four dots is odd, while g shows wide minima for even $N_e \simeq 2, 4, 6$. The local charge N_e shows a staircase-like behavior as a function of ϵ_d . Among the conductance minima, the one around half-filling $N_e \simeq 4$ becomes quite wide because of the Mott-Hubbard behavior. The feature of the conductance near half-filling depends on whether the number of quantum dots is even or odd, and in the case of the triple dots the Kondo resonance emerging at the Fermi level contributes to the tunneling of the Unitary limit.

This paper is organized as follows. In Sec. II, we describe the outline of the formulation to deduce the conductance from the fixed-point energy levels of the NRG. In Sec. III, we show the calculated results. In Sec. IV, discussion are given.

II. MODEL AND FORMULATION

In this section, we describe the outline of the method to deduce the phase shifts, which determine the ground-state of the system, from the fixed-point Hamiltonian of NRG.²¹ This approach requires only the energy eigen-

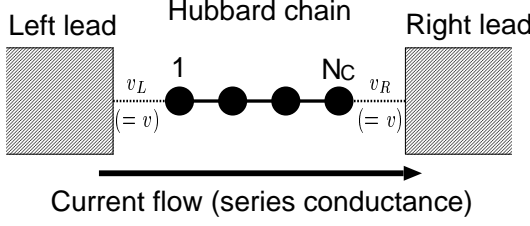


FIG. 1: Schematic picture of a series connection.

values, and thus it can be carried out easier than the calculations of some correlation functions.

We start with a Hubbard chain of a finite size N_c which is connected to two non-interacting leads at the left(L) and right(R) by the tunneling matrix elements v_L and v_R , respectively, as illustrated in Fig. 1. The Hamiltonian is given by

$$\mathcal{H} = \mathcal{H}_C^0 + \mathcal{H}_C^U + \mathcal{H}_{\text{mix}} + \mathcal{H}_{\text{lead}} \quad (1)$$

with

$$\begin{aligned} \mathcal{H}_C^0 = & -t \sum_{i=1}^{N_c-1} \sum_{\sigma} \left(d_{i\sigma}^\dagger d_{i+1\sigma} + d_{i+1\sigma}^\dagger d_{i\sigma} \right) \\ & + \epsilon_d \sum_{i=1}^{N_c} \sum_{\sigma} d_{i\sigma}^\dagger d_{i\sigma}, \end{aligned} \quad (2)$$

$$\mathcal{H}_C^U = U \sum_{i=1}^{N_c} d_{i\uparrow}^\dagger d_{i\uparrow} d_{i\downarrow}^\dagger d_{i\downarrow}, \quad (3)$$

$$\begin{aligned} \mathcal{H}_{\text{mix}} = & v_L \sum_{\sigma} \left(d_{1,\sigma}^\dagger \psi_{L\sigma} + \psi_{L\sigma}^\dagger d_{1,\sigma} \right) \\ & + v_R \sum_{\sigma} \left(\psi_{R\sigma}^\dagger d_{N_c,\sigma} + d_{N_c,\sigma}^\dagger \psi_{R\sigma} \right), \end{aligned} \quad (4)$$

$$\mathcal{H}_{\text{lead}} = \sum_{\nu=L,R} \sum_{k\sigma} \epsilon_{k\nu} c_{k\nu\sigma}^\dagger c_{k\nu\sigma}, \quad (5)$$

where $d_{i\sigma}$ annihilates an electron with spin σ at site i in the Hubbard chain, which is characterized by the nearest-neighbor hopping matrix element t , onsite energy ϵ_d , and Coulomb interaction U . In the lead at ν ($= L, R$), the operator $c_{k\nu\sigma}^\dagger$ creates an electron with energy $\epsilon_{k\nu}$ corresponding to an one-particle state $\phi_{k\nu}(r)$. The linear combinations of the conduction electrons $\psi_{L\sigma}$ and $\psi_{R\sigma}$ mixed with the electrons in the interacting site labeled by $i = 1$ and N_c , respectively, where $\psi_{\nu\sigma} = \sum_k c_{k\nu\sigma} \phi_{k\nu}(r_\nu)$ and r_ν is the position at the interface in the lead ν . We assume that the hybridization strength $\Gamma_\nu \equiv \pi v_\nu^2 \sum_k |\phi_{k\nu}(r_\nu)|^2 \delta(\omega - \epsilon_{k\nu})$ is a constant independent of the frequency ω , and take the origin of the energy to be $\mu = 0$.

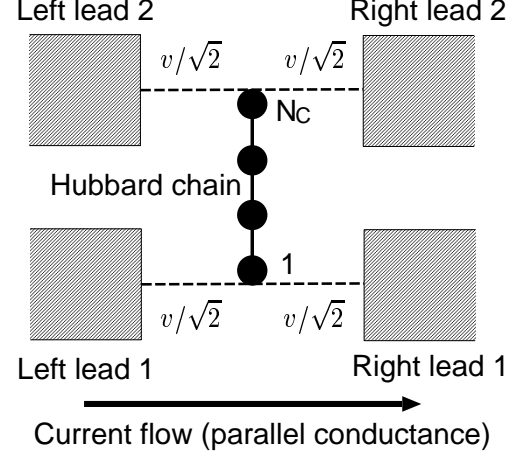


FIG. 2: Schematic picture of a parallel connection.

A. Ground-state properties and phase shifts

In the following, we assume that the system has an inversion symmetry, $v_L = v_R$ ($\equiv v$) and $\Gamma_L = \Gamma_R$ ($\equiv \Gamma$). In this case, the orbitals which have even and odd parities can be introduced as

$$a_{j,\sigma} = \frac{d_{j,\sigma} + d_{N_c-j+1,\sigma}}{\sqrt{2}}, \quad (6)$$

$$b_{j,\sigma} = \frac{d_{j,\sigma} - d_{N_c-j+1,\sigma}}{\sqrt{2}}, \quad (7)$$

where $j = 1, 2, \dots, N_c/2$ for even N_c , while for odd N_c there exists one extra unpaired orbital $a_{(N_c+1)/2,\sigma} \equiv d_{(N_c+1)/2,\sigma}$ in addition to the pairs for $j = 1, 2, \dots, (N_c-1)/2$. Due to the inversion symmetry, at zero temperature $T = 0$ and Fermi energy $\omega = 0$, the retarded Green's functions for $a_{1,\sigma}$ and $b_{1,\sigma}$ can be written in the forms,²¹

$$\langle\langle a_{1,\sigma}; a_{1,\sigma}^\dagger \rangle\rangle_{\omega=0} = \frac{1}{\Gamma} \frac{1}{\kappa_{\text{even}} + i} \equiv \frac{1}{\Gamma} \frac{-e^{i\delta_{\text{even}}}}{\sqrt{\kappa_{\text{even}}^2 + 1}}, \quad (8)$$

$$\langle\langle b_{1,\sigma}; b_{1,\sigma}^\dagger \rangle\rangle_{\omega=0} = \frac{1}{\Gamma} \frac{1}{\kappa_{\text{odd}} + i} \equiv \frac{1}{\Gamma} \frac{-e^{i\delta_{\text{odd}}}}{\sqrt{\kappa_{\text{odd}}^2 + 1}}. \quad (9)$$

Namely, each of these two retarded Green's functions is determined by a single parameter, κ_{even} or κ_{odd} , which contains all effects of the scatterings and interactions. Furthermore, the phase shifts for the even and odd partial waves, δ_{even} and δ_{odd} , correspond to the phase of these two Green's functions in the complex plane.

The two phase shifts, δ_{even} and δ_{odd} , determine the ground-state properties of the series connection illustrated in Fig. 1.²⁴ Specifically, based on the Kubo formalism and Friedel sum rule, the dc conductance g_{series} and total number of electrons in the Hubbard chain

$N_{\text{el}} \equiv \sum_{i=1}^{N_C} \sum_{\sigma} \langle d_{i\sigma}^{\dagger} d_{i\sigma} \rangle$ can be expressed in the forms,²¹

$$g_{\text{series}} = \frac{2e^2}{h} \sin^2(\delta_{\text{even}} - \delta_{\text{odd}}), \quad (10)$$

$$N_{\text{el}} = \frac{2}{\pi} (\delta_{\text{even}} + \delta_{\text{odd}}). \quad (11)$$

The description based on the phase shifts can be justified when the imaginary of the $N_C \times N_C$ matrix version of the retarded self-energy due to the interaction \mathcal{H}_C^U vanishes, $\text{Im } \Sigma^+(0) = 0$, at $T = 0$ and $\omega = 0$.^{21,23}

Furthermore, from these two phase shifts defined with respect to the series connection, one can deduce the parallel conductance g_{parallel} for the current flowing in the horizontal direction in the geometry illustrated in Fig. 2;

$$g_{\text{parallel}} = \frac{2e^2}{h} (\sin^2 \delta_{\text{even}} + \sin^2 \delta_{\text{odd}}). \quad (12)$$

This expression can be derived from the Kubo formula,²¹ and is equivalent to the multi-channel version of the Landauer formula.^{25,26} For the parallel conductance, there are two conducting channels that can contribute to the total current, so that the maximum value of g_{parallel} becomes $4e^2/h$. Specifically, in the parallel connection in Fig. 2, the tunneling matrix elements between the leads and interacting part are taken to be $v/\sqrt{2}$. In this case, because of the inversion symmetry between left lead 1 (2) and right lead 1 (2), an odd combination of the states from these two leads is separated, and the interacting site for $i = 1$ ($i = N_C$) is coupled to an even combination by the matrix element v . Therefore, the ground state properties for the parallel geometry can be related to the phase shifts δ_{even} and δ_{odd} that are defined with respect to the series connection in eqs. (8) and (9). Particularly, N_{el} for parallel connection is equal to that for the series connection, which is given by eq. (11).

B. Fixed-point Hamiltonian and phase shifts

The two phase shifts δ_{even} and δ_{odd} can be deduced from the fixed-point eigenvalues NRG. In this approach, a sequence of the Hamiltonian H_N is introduced, by carrying out the logarithmic discretization for the conduction band with the half-width D ,^{15,16,17} as

$$H_N = \Lambda^{(N-1)/2} \left(\mathcal{H}_C^0 + \mathcal{H}_C^U + H_{\text{mix}} + H_{\text{lead}}^{(N)} \right), \quad (13)$$

$$H_{\text{mix}} = \bar{v} \sum_{\sigma} \left(f_{0,L\sigma}^{\dagger} d_{1,\sigma} + d_{1,\sigma}^{\dagger} f_{0,L\sigma} \right) + \bar{v} \sum_{\sigma} \left(f_{0,R\sigma}^{\dagger} d_{N_C,\sigma} + d_{N_C,\sigma}^{\dagger} f_{0,R\sigma} \right), \quad (14)$$

$$H_{\text{lead}}^{(N)} = D \frac{1+1/\Lambda}{2} \sum_{\nu=L,R} \sum_{\sigma} \sum_{n=0}^{N-1} \xi_n \Lambda^{-n/2} \times \left(f_{n+1,\nu\sigma}^{\dagger} f_{n,\nu\sigma} + f_{n,\nu\sigma}^{\dagger} f_{n+1,\nu\sigma} \right), \quad (15)$$

where $\bar{v} = \sqrt{2D\Gamma A_{\Lambda}/\pi}$, $A_{\Lambda} = \frac{1}{2} \frac{1+1/\Lambda}{1-1/\Lambda} \log \Lambda$, and

$$\xi_n = \frac{1-1/\Lambda^{n+1}}{\sqrt{1-1/\Lambda^{2n+1}} \sqrt{1-1/\Lambda^{2n+3}}}. \quad (16)$$

The low-lying eigenvalues of H_N for the finite Hubbard chain also converge, for large N , to the fixed-point values which have one-to-one correspondence to the energy spectrum of a local Fermi liquid,^{20,21} as that in the case of the single Anderson (or Kondo) impurity.^{15,16,17} The fixed-point Hamiltonian, which describes the free quasi-particles, is given by

$$H_{\text{qp}}^{(N)} = \Lambda^{(N-1)/2} \left(H_C^{\text{eff}} + H_{\text{mix}} + H_{\text{lead}}^{(N)} \right), \quad (17)$$

where $H_C^{\text{eff}} \equiv \mathcal{H}_C^0 + \sum_{i,j=1}^{N_C} \text{Re } \Sigma_{ij}^+(0) d_{i\sigma}^{\dagger} d_{j\sigma}$. The many-body corrections enter through the real part of self-energy at $T = 0$, $\omega = 0$. However, instead of calculating the self-energy directly with NRG, one can determine accurately the quasi-particle energies ε_{γ}^* with parity γ (= “even” or “odd”) from the fixed-point eigenvalues of the discretized Hamiltonian H_N . The phase shifts δ_{even} and δ_{odd} defined in eqs. (8) and (9) can be obtained via the parameter κ_{γ} which can be deduced from the quasi-particle energy ε_{γ}^* ,²¹

$$\kappa_{\gamma} = (\bar{v}^2/\Gamma D) \lim_{N \rightarrow \infty} D \Lambda^{(N-1)/2} g_N(\varepsilon_{\gamma}^*). \quad (18)$$

Here, $g_N(\omega) = \sum_{m=0}^N |\varphi_m(0)|^2 / (\omega - \epsilon_m)$ is the Green’s function for one of the isolated leads described in $H_{\text{lead}}^{(N)}$, and ϵ_m and $\varphi_m(n)$ are the corresponding eigenvalue and eigenfunction for $0 \leq n \leq N$.

III. RESULTS FOR A FOUR-DOT ARRAY

In this section, we apply the formulation described in the above to the four-site Hubbard chain, $N_C = 4$, attached to the reservoirs. To construct the Hilbert space for H_{N+1} from that of H_N , we introduce the two orbitals $f_{N+1,R\sigma}^{\dagger}$ and $f_{N+1,L\sigma}^{\dagger}$. Then, we keep the lowest 1716 eigenstates for constructing the Hilbert space for the next step. With this procedure, the discretized Hamiltonian H_N that consists of $2(N+1) + N_C$ sites can be diagonalized exactly up to $N = 0$ for $N_C = 4$. For $N \geq 1$, we have checked that the conductance of the noninteracting case $U = 0$ are reproduced sufficiently well with this procedure also for a rather large value of the discretization parameter $\Lambda = 6.0$. The results of the fixed-point eigenvalues of H_N can be reproduced by the quasi-particle Hamiltonian for all the cases we have examined. It justifies the assumption of the local Fermi liquid we have made in the previous section.

A. Conductance for the series connection

We now show the onsite energy ϵ_d dependence of the conductance for the series connection. The onsite energy

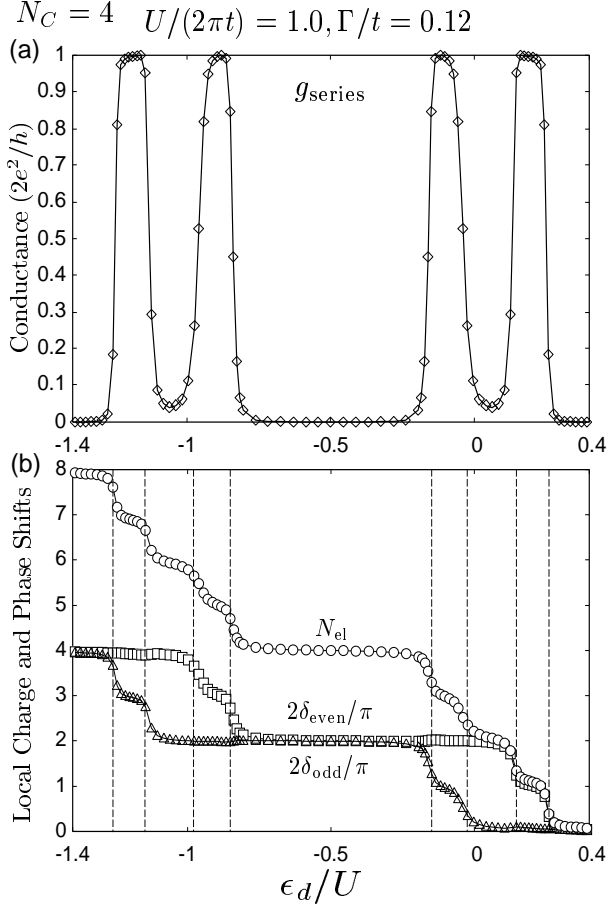


FIG. 3: (a) The conductance g_{series} , (b) the local charge N_{el} , the phase shifts $2\delta_{\text{even}}/\pi$ and $2\delta_{\text{odd}}/\pi$ as functions of ϵ_d/U for $U/(2\pi t) = 1.0$, $\Gamma/t = 0.12$, $t/D = 0.1$, and $\Lambda = 6.0$. The dashed vertical lines in (b) show the values of ϵ_d at which N_{el} jumps in the limit $\Gamma = 0$.

ϵ_d can be controlled by the gate voltage in real quantum dots systems. In Fig. 3, (a) the conductance g_{series} for series connection, (b) total charge N_{el} in the four-site Hubbard chain, the phase shifts δ_{even} and δ_{odd} are plotted as functions of ϵ_d/U for $U/(2\pi t) = 1.0$, $\Gamma/t = 0.12$, $t/D = 0.1$ and $\Lambda = 6.0$. The vertical dashed lines in (b) correspond to the values of ϵ_d at which N_{el} jumps discontinuously in the limit of $\Gamma \rightarrow 0$. The conductance shows wide maxima in the regions of ϵ_d for odd occupations $N_{\text{el}} \simeq 1, 3, 5, 7$. In these regions, the phase shifts behave as $\delta_{\text{even}} - \delta_{\text{odd}} \simeq \pi/2$. These broad maxima with $g \simeq 2e^2/h$ are the Kondo behavior of the conductance. In contrast, the conductance shows minima for even occupations $N_{\text{el}} \simeq 2, 4, 6$. In this case, the phase shifts behave as $\delta_{\text{even}} - \delta_{\text{odd}} \simeq 0$ or π . Among the three conductance valleys, the one around the half-filling has a different feature from the others. This difference is caused by the Coulomb interaction U . The width of the valley around the half-filling becomes quite large owing to a tendency towards a development of a Mott-Hubbard insulating gap due to Coulomb interaction U . We discuss

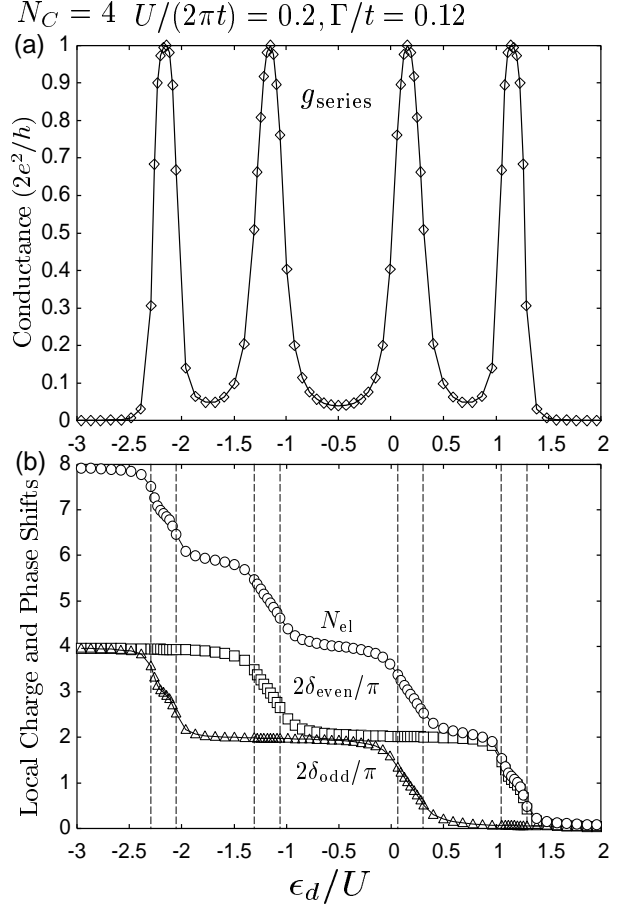


FIG. 4: (a) The conductance g_{series} , (b) the local charge N_{el} , the phase shifts $2\delta_{\text{even}}/\pi$ and $2\delta_{\text{odd}}/\pi$ as functions of ϵ_d/U for $U/(2\pi t) = 0.2$, $\Gamma/t = 0.12$, $t/D = 0.1$, and $\Lambda = 6.0$. The dashed vertical lines in (b) show the values of ϵ_d at which N_{el} jumps in the limit $\Gamma = 0$.

the behavior of the conductance around half-filling in detail later. In the case of the data shown in Fig. 3, the hybridization Γ is relatively small compared to the hopping matrix element t . It corresponds to the situation that the level-broadening caused by the tunneling matrix elements between the chain and the leads is small. Therefore, the local charge N_{el} shows a step behavior near the dashed lines, and it jumps discontinuously in the limit of $\Gamma \rightarrow 0$. For interacting electrons, the step emerges also for odd $N_{\text{el}} = 1, 3, 5$, and 7, at which one of the phase two shifts changes the value by $\pi/2$. When the onsite potential ϵ_d/U decreases from 0.4 to 0, the phase shift for the even partial wave δ_{even} increases from 0 to π via two successive $\pi/2$ steps, while the phase shifts for odd partial wave δ_{odd} remains almost unchanged at 0. Then, in the region of $-0.5 < \epsilon_d/U < 0.0$, the phase shift for the odd part δ_{odd} shows one $\pi/2$ step, while the even one remains to be constant $\delta_{\text{even}} \simeq \pi$. Similar features are seen also in the region of $\epsilon_d/U < -0.5$, where the results have been deduced from those obtained for $-0.5 < \epsilon_d/U < 0.4$ via an electron-hole transformation

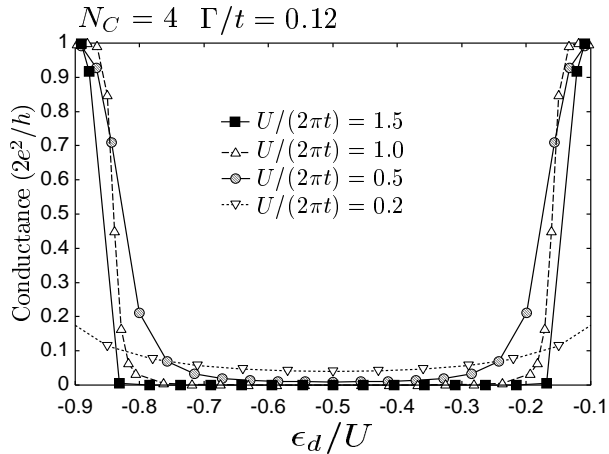


FIG. 5: The behavior of the conductance around half-filling for $U/(2\pi t) = 0.2, 0.5, 1.0$ and 1.5 . Here, $\Gamma/t = 0.12$, $t/D = 0.1$, and $\Lambda = 6.0$.

for \mathcal{H} defined in eq. (1). In the series of the quantum-dot array, the resonance state for the even partial wave and that for the odd partial wave cross the Fermi level alternatively when ϵ_d is varied. It reflects the behavior of the phase shifts mentioned above.

We next examine the situation where the Coulomb interaction is much smaller than that in the case considered in the above. The calculated results for $U/(2\pi t) = 0.2$ are shown in Fig. 4, where $\Gamma/t = 0.12$ and $t/D = 0.1$. The conductance g shows wide minima and maxima alternatively as a function of ϵ_d . Particularly, the conductance maxima becomes very narrow, and the features of the peaks is similar to that for non-interacting systems $U = 0$. Nevertheless, the shape of the conductance peaks seen in Fig. 4 deviates from the simple Lorentzian shape as a result of the many-body effects. In this small U case, the local charge N_{el} becomes flat only for even occupancies $N_{\text{el}} = 2, 4, 6$, and it means that two electrons occupy the resonance state almost simultaneously when it passes through the Fermi level. Correspondingly, the phase shifts δ_{even} and δ_{odd} do not show the clear $\pi/2$ steps, although some weak structures for the development of the $\pi/2$ steps are seen, especially for $N_{\text{el}} = 1, 7$. The valley around half-filling $N_{\text{el}} \simeq 4$ is slightly wider than the ones at $N_{\text{el}} \simeq 2$ and 6 , but the difference is not so large in this small U case.

In order to investigate the Mott-Hubbard behavior near half-filling, $\epsilon_d/U = -0.5$, the conductance is plotted for several values of $U/(2\pi t) = 0.2, 0.5, 1.0$ and 1.5 in Fig. 5, where the other parameters are chosen to be $\Gamma/t = 0.12$, $t/D = 0.1$, and $\Lambda = 6.0$. As U increases, the feature of the valley approaching to the one for the real insulating gap in the thermodynamic limit $N_C \rightarrow \infty$. Namely, the two edges of the conductance valley become sharper. The value of the conductance at the valley decreases exponentially with increasing U .²⁰ The NRG results show that the low-energy states at the fixed-point can be mapped onto the quasi-particle excitations of the

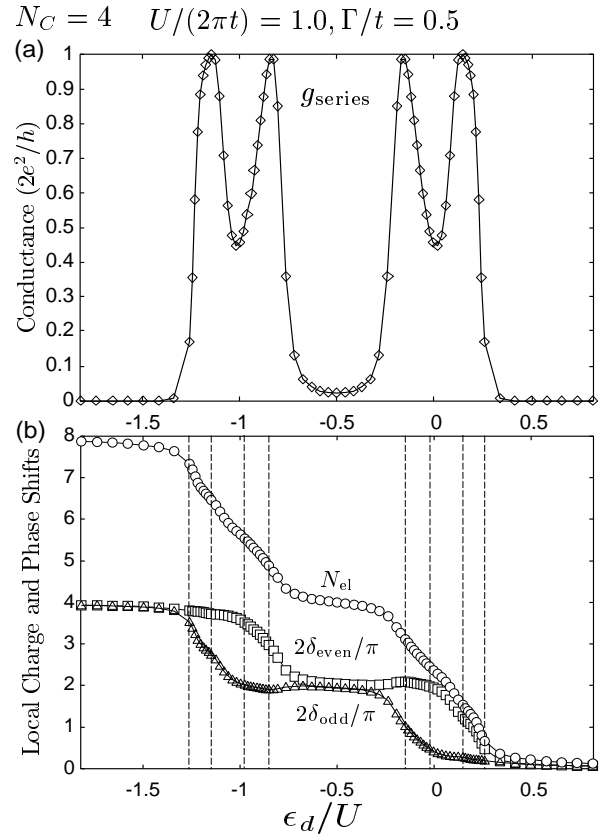


FIG. 6: (a)The conductance g_{series} , (b)the local charge N_{el} , the phase shifts $2\delta_{\text{even}}/\pi$ and $2\delta_{\text{odd}}/\pi$ as functions of ϵ_d/U for $U/(2\pi t) = 1.0$, $\Gamma/t = 0.5$, $t/D = 0.02$, and $\Lambda = 6.0$. The dashed vertical lines in (b) show the values of ϵ_d at which N_{el} jumps in the limit $\Gamma = 0$.

local Fermi liquid. This is because the size of the number of the quantum dots N_C is finite, and the array is connected to the noninteracting leads with continuous energy spectrum. Therefore, although the value of the conductance near half-filling is very small, the ground state is not a real insulator but a highly renormalized state similar to that of the heavy fermions.

So far, the hybridization energy scale Γ is taken to be much smaller than the hopping matrix element t between the dots, $\Gamma/t = 0.12$. In order to see how the couplings between the quantum-dot array and leads change the ground-state properties, we have carried out the calculations taking the hybridization to be $\Gamma/t = 0.5$. The results are show in Fig. 6 for $U/(2\pi t) = 1.0$, $t/D = 0.02$ and $\Lambda = 6.0$. The local charge N_{el} , which shows a staircase behavior for small Γ as seen in Fig. 3, becomes a gentle slope in Fig. 6 (b). The conductance plateaus become round, and the valleys become shallow. This is because the large hybridization makes the resonance peaks broad, and it reduces the correlation effects. The conductance valley around the half-filling is deeper than the other two valleys owing to the Mott-Hubbard behavior.

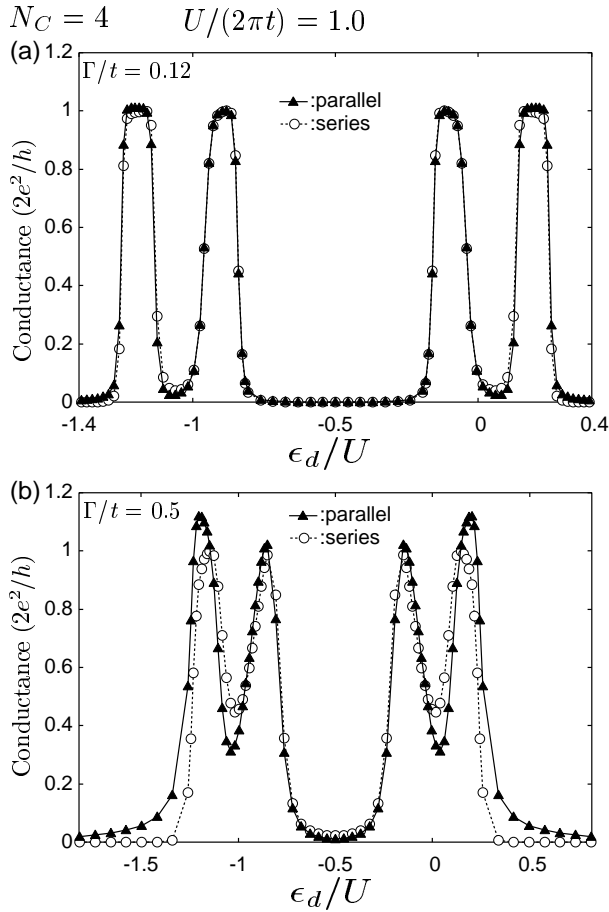


FIG. 7: The conductance in the series (solid line) and parallel (dotted line) connections for interacting electrons $U/(2\pi t) = 1.0$ as functions of ϵ_d/U , where (a) $\Gamma/t = 0.12$, $t/D = 0.1$ and (b) $\Gamma/t = 0.5$, $t/D = 0.02$.

B. Conductance for the parallel connection

We have also calculated the parallel conductance using eq. (12) and the results of the phase shifts for the series connection presented above. The series and parallel conductances for $U/(2\pi t) = 1.0$ are plotted in Fig. 7 as functions of ϵ_d/U for two different values of the hybridization, (a) $\Gamma/t = 0.12$ and (b) $\Gamma/t = 0.5$. For small Γ , the value of the parallel conductance is almost the same as that of the series conductance, as seen in Fig. 7 (a). The difference becomes larger, however, for large Γ , as seen in the lower panel (b). The valleys of the conductance are deeper for the parallel connection than that of the series connection. This seems to be caused by the fact the even and odd parts of the partial waves contribute to the parallel conduction separately through eq. (12). The parallel conductance for large Γ , (b), is slightly larger than $2e^2/h$ around the first and fourth maxima. As mentioned in the previous section, the upper bound of the parallel conductance is $2e^2/h \times 2$, because two conducting channels can contribute to the current in the geometry shown in Fig. 2. For the quantum-dot chain consisting

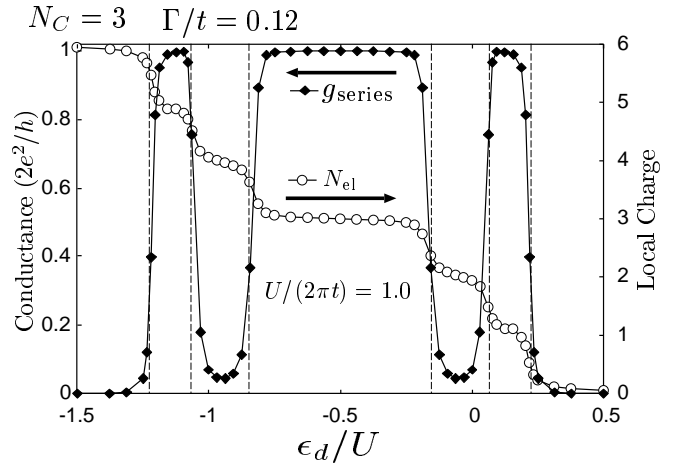


FIG. 8: NRG results for the conductance g_{series} and local charge N_{el} for triple dots $N_C = 3$ as functions of ϵ_d/U for $U/(2\pi t) = 1.0$, $\Gamma/t = 0.12$, $t/D = 0.1$, and $\Lambda = 6.0$. The dashed vertical lines show the values of ϵ_d at which N_{el} jumps in the limit $\Gamma = 0$.

of four sites, the parallel conductance does not reach the upper bound, and a similar feature has also been confirmed to be seen for the triple dots.²¹ In the case of the one-dimensional array of quantum dots, the Kondo resonances caused by different orbitals pass through the Fermi level alternatively, when ϵ_d is varied. Therefore, only one of the two partial waves, even or odd, can contribute to the tunneling current, so that at the maxima the parallel conductance becomes about $2e^2/h$ despite in the presence of the two conducting channels. To reach the upper bound, the quantum-dot systems are required to have a degeneracy in the discrete energy levels. It is not the case of the one-dimensional array.

IV. DISCUSSION

The Mott-Hubbard insulating behavior is seen around half-filling in the conductance through the one-dimensional array consisting of the even number of quantum dots N_C , as discussed in Sec. III. The situation is quite different for the array with odd N_C , because the Kondo resonance contributes to the current as shown in Fig. 8, where the series conductance and total charge N_{el} in triple dots ($N_C = 3$) are plotted as functions of ϵ_d/U .²¹ Around half-filling, the conductance shows a plateau $g_{\text{series}} \simeq 2e^2/h$ in stead of a wide gap Δ_{gap} as seen in Fig. 5 for even N_C . However, Kondo temperature T_K decreases with increasing U ,²⁰ and thus the Kondo plateau can be observed only at low temperatures $T \lesssim T_K$. If the single-particle spectral function is calculated at half-filling as a function of frequency ω , the narrow Kondo peak will be seen at $0 < |\omega| \lesssim T_K$. Then, there will be a pseudo-gap region $T_K \lesssim |\omega| < \Delta_{\text{gap}}$, in which the spectral weight almost vanishes. The plateau becomes wider with increasing U ,²¹ and the width is de-

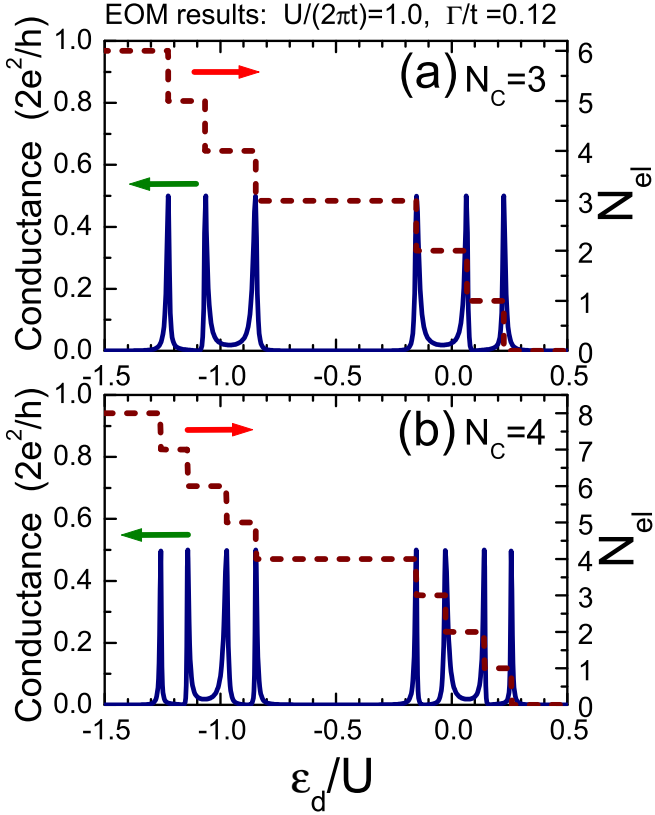


FIG. 9: EOM (equation of motion) results for the series conductance for the quantum-dot array of the size (a) $N_C = 3$ and (b) $N_C = 4$ obtained from eq. (20), where $U/(2\pi t) = 1.0$ and $\Gamma/t = 0.12$. The results describe a typical feature of a Coulomb oscillation at high temperatures $T_K \ll T \ll U$. The dashed lines show the local charge N_{el} in the isolated *molecule* for $\Gamma = 0$.

terminated by the charge excitation gap $2\Delta_{\text{gap}}$. Alternatively, one can estimate the excitation gap from the width of the plateau of the conductance.

So far, we have concentrated on the transport properties at zero temperature. For comparison, we now consider the conductance at high temperatures. For qualitatively understanding of the physics at high-energy energy scale, the equation motion (EOM) method can be used.²⁷ It is equivalent basically to the Hubbard I approximation,²⁸ and in the present case we start with a *molecule limit*, where $\Gamma = 0$ and then the quantum-dot array can be regarded like an artificial *molecule* described by the Hamiltonian $\mathcal{H}_C^0 + \mathcal{H}_C^U$ defined in eqs. (2) and (3). With this method, the full Green's function $G_{ij}^{(\text{EOM})}(\omega)$ is obtained by substituting the self-energy defined with respect to the *molecule* $\Sigma_{ij}^{(\text{mol})}(\omega)$, which is calculated ex-

actly, into the $N_C \times N_C$ matrix Dyson equation,

$$\left\{ \mathbf{G}^{(\text{EOM})}(\omega) \right\}^{-1} = \left\{ \mathbf{G}^{(0)}(\omega) \right\}^{-1} - \Sigma^{(\text{mol})}(\omega). \quad (19)$$

Here, $\mathbf{G}^{(0)}(\omega) = \{G_{ij}^{(0)}(\omega)\}$ is the noninteracting Green's function defined with respect to the whole system including the two leads, and is determined by the Hamiltonian $\mathcal{H}_C^0 + \mathcal{H}_{\text{mix}} + \mathcal{H}_{\text{lead}}$. Then, a typical value of the conductance at high-temperatures $T_K \ll T \ll U$ is estimated by using an approximate formula following Kawabata,²⁴

$$g_{\text{series}} \sim \frac{e^2}{h} \times 4\Gamma^2 \left| G_{N_C 1}^{(\text{EOM})}(0) \right|^2, \quad (20)$$

where a factor 1/2 has been introduced phenomenologically taking into account the high-energy behavior that the resonance tunneling using the Hubbard band occurs not simultaneously for the up and down spin components. In Fig. 9, the conductance obtained from eq. (20) is plotted for (a) $N_C = 3$ and (b) $N_C = 4$, where the same parameter value is chosen for U and Γ as those in Figs. 8 and 3. At high temperatures, the conductance almost vanishes both for even and odd N_{el} . The peaks of the Coulomb oscillation appear at the values of ϵ_d , where N_{el} jumps discontinuously by an addition of one electron. If the temperature decreases, the bottom of the valleys at odd N_{el} will rise, and it develops at $T \lesssim T_K$ to form the Kondo plateaus of the Unitary limit which we have described in the previous section. Particularly, the wide gap around half-filling for the triple dots in Fig. 9 (a) evolves to the broad plateau in Fig. 8.

In summary, we have studied the ground-state properties of an array consisting of four quantum dots based on a Hubbard chain attached to two non-interacting leads. Using NRG approach, we have deduced the phase shifts, by which the conductance and local charge away from half-filling can be determined, from the low-energy eigenvalues near the Fermi-liquid fixed-point. We have also discussed the parallel conductance of the quantum dot array connected transversely to four leads. Our formulation to calculate the two phase shifts for even and odd partial waves is quite general, and will be applied to various quantum-dot systems in the Kondo regime.

Acknowledgments

The authors are grateful to A. C. Hewson for valuable discussions. Numerical computation was partly carried out using Computer Facility of Yukawa Institute.

¹ L. I. Glazman and M. E. Raikh, JETP Lett. **47**, 452 (1988).

² T. K. Ng and P. A. Lee, Phys. Rev. Lett. **61**, 1768 (1988).

³ D. Goldhaber-Gordon, H. Shtrikman, D. Mahalu, D. Abusch-Magder, U. Meirav, and M. A. Kastner, Nature

³ **391**, 156 (1998).

⁴ S. M. Cronenwett, T. H. Oosterkamp, and L. P. Kouwenhoven: *Science* **281**, 540 (1998).

⁵ W. Izumida, O. Sakai, and Y. Shimizu, *J. Phys. Soc. Jpn.* **66**, 717 (1998).

⁶ W. Hofstetter, J. König, and H. Schoeller: *Phys. Rev. Lett.* **87**, 156803 (2001).

⁷ K. Kobayashi, H. Aikawa, S. Katsumoto, and Y. Iye: *Phys. Rev. Lett.* **88**, 256806 (2002).

⁸ A. V. Rozhkov and D. P. Arovas, *Phys. Rev. Lett.* **82**, 2788 (1999).

⁹ A. A. Clerk and V. Ambegaokar, *Phys. Rev. B* **61**, 9109 (2000).

¹⁰ M.-S Choi, M. Lee, K. Kang, and W. Belzig, *Phys. Rev. B* **70**, 020502(R) (2004).

¹¹ A. Oguri, Y. Tanaka, and A. C. Hewson, *J. Phys. Soc. Jpn.* **73**, 2494 (2004).

¹² V. Meden, S. Andergassen, W. Metzner, U. Schollwöck and K. Schönhammer, *Europhys. Lett.* **64**, 769 (2003).

¹³ R. A. Molina, D. Weinmann, R.A.Jalabert, G.-L. Ingold, and J. -L. Pichard, *Phys. Rev. B* **67**, 235306 (2003).

¹⁴ T. Rejec and A. Ramšak, *Phys. Rev. B* **68**, 035342 (2003).

¹⁵ K. G. Wilson, *Rev. Mod. Phys.* **47**, 773 (1975).

¹⁶ H. R. Krishna-murthy, J. W. Wilkins, and K. G. Wilson, *Phys. Rev. B* **21**, 1003 (1980).

¹⁷ H. R. Krishna-murthy, J. W. Wilkins, and K. G. Wilson, *Phys. Rev. B* **21**, 1044 (1980).

¹⁸ W. Izumida, O. Sakai, and Y. Shimizu: *J. Phys. Soc. Jpn.* **67**, 2444 (1998).

¹⁹ W. Izumida and O. Sakai *Phys. Rev. B* **62**, 10260 (2000).

²⁰ A. Oguri and A. C. Hewson, *J. Phys. Soc. Jpn.* **74**, 988 (2005).

²¹ A. Oguri, Y. Nisikawa and A. C. Hewson, *J. Phys. Soc. Jpn.* **74**, 2554 (2005).

²² A. Oguri, *Phys. Rev. B* **63**, 115305 (2001); *ibid.* [Errata: **63**, 249901 (2001)].

²³ A. Oguri, *J. Phys. Soc. Jpn.* **70**, 2666 (2001); *ibid.* **72**, 3301 (2003).

²⁴ A. Kawabata, *J. Phys. Soc. Jpn.* **60**, 3222 (1991).

²⁵ M. Büttiker and Y. Imry and R. Landauer and S. Pinhas, *Phys. Rev. B* **31**, 6207 (1985).

²⁶ Y. Tanaka, A. Oguri, and H. Ishii, *J. Phys. Soc. Jpn.* **71**, 211 (2002).

²⁷ Y. Meir, N. S. Wingreen, and P. A. Lee, *Phys. Rev. Lett.* **66**, 3048 (1991).

²⁸ J. Hubbard, *Proc. Roy. Soc. A* **276**, 238 (1963).